CORONAS-F/SPIRIT EUV observations of October–November 2003 solar eruptive events in combination with SOHO/EIT data

V. V. Grechnev[1], I. M. Chertok[2], V. A. Slemzin[3], S. V. Kuzin[3],
A. P. Ignat'ev[3], A. A. Pertsov[3], I. A. Zhitnik[3],
J.-P. Delaboudinière[4], F. Auchère[4]

[1]*Institute of Solar-Terrestrial Physics SB RAS, Irkutsk, Russia*
[2]*IZMIRAN, Troitsk, Moscow Region, 142190 Russia*
[3]*Lebedev Institute of Physics, Leninskii Pr. 53, Moscow, 117924 Russia*
[4]*Institut 'd Astrophysique Spatiale, Orsay, France*

Abstract

The extraordinary solar activity of October–November 2003 manifested itself in many powerful eruptive events, including large CMEs and extremely powerful flares. A number of major events were accompanied by practically all known phenomena of the solar activity, both local and large-scale, and caused severe space weather disturbances. We study large-scale post-eruptive activity manifestations on the Sun associated with CMEs, i.e., dimmings and coronal waves, observed in extreme ultraviolet with the SPIRIT on the CORONAS-F and the EIT telescope on the SOHO spacecrafts. During that period, observations with a cadence of 15 to 45 minutes were carried out by the SPIRIT in the 175 Å and 304 Å bands simultaneously. The EIT observed with 12-min cadence in the 195 Å band as well as with 6-hour cadence in the 171, 284, and 304 Å bands. These data complement each other both in the temporal and spectral coverage. Our analysis reveals that largest-scale dimmings covered almost the whole southern part of the Sun's visible side and exhibited homology, with one homological structure being changed to another configuration on October 28. These structures show connections between large superactive and smaller regions that constituted a huge activity complex responsible for the extraordinary solar activity of that period. Coronal waves were observed at 175 Å as well as at 195 Å in some events, in areas where there were no active regions, but in the 175 Å images they look fainter. They were not accompanied by deep, long-living dimmings. By contrast, such dimmings were observed in active regions, in their vicinity, and between them. These facts rule out the direct relation of the phenomena of long-term dimmings and coronal waves. On November 18, a motion of an ejecta was observed at the solar disk as a propagation of a dark feature only in the 304 Å band, which can be interpreted as an absorption in a "cloud" formed from material of the eruptive filament, which probably failed to become a CME core.

1 Introduction

A series of extreme events that occurred in October–November 2003 is a subject of comprehensive investigations of both violent solar activity and severe space weather disturbances [e.g., *Veselovsky et al.*, 2004, *Yermolaev et al.*, 2005, and papers of this issue]. In particular, *Chertok and Grechnev* [2005, hereafter referred to as Paper I] studied large-scale manifestations of the solar activity by full-disk heliograms gathered with the Extreme ultraviolet Imaging Telescope (EIT) [*Delaboudinière et al.*, 1995] aboard the Solar and Heliospheric Observatory (SOHO). They analyzed extended dimmings, i.e. regions of temporarily reduced brightness (we do not apply the widely used term *transient coronal holes* to avoid confusion between decreased brightness and open magnetic structures) and, to lesser extent, coronal waves (bright propagating or quasi-stationary fronts) associated with halo coronal mass ejections (CMEs) and powerful flares. Such phenomena have been studied previously by, for example, *Hudson and Webb* [1997], *Thompson et al.* [1998], *Zarro et al.* [1999], *Gopalswamy and Thompson* [2000], *Hudson and Cliver* [2001]. The events under consideration took place during two passages across the visible disk of three big highly active (*superactive*) regions: AR 484 (501 at the second rotation, Carrington latitude and longitude N04, 354), AR 486/508 (S15, 283), and AR 488/507 (N08, 291).

In this paper, we continue the analysis of the October–November 2003 large-scale solar surface activity based on extreme-ultraviolet (EUV) observations with the **SP**ectrograph**I**c X-**R**ay **I**maging **T**elescope-spectroheliograph

(SPIRIT) [*Zhitnik et al.*, 2002] aboard the CORONAS-F space solar observatory [*Oraevsky and Sobelman*, 2002; *Oraevsky et al.*, 2003] launched in August 2001. Combining CORONAS-F/SPIRIT 175 Å & 304 Å and SOHO/EIT 195, 171, 304, and 284 Å data, and taking advantage of the fact that observations of these two telescopes are complementary in the sense of the spectral and temporal coverage, we endeavor to obtain still more comprehensive picture of the large-scale surface activity associated with CMEs during that extraordinary period.

The present results and conceptions on the origination of dimmings are as follows. The coincidence of long-living dimmings observed in many events in different-temperature coronal lines and in the 304 Å transition-region band [*Chertok and Grechnev, 2003b*] provides support for their origination due to plasma density depletion in the low corona [see, e.g., *Thompson et al.*, 1998; *Zarro et al.*, 1999; *Harrison et al.*, 2003], sometimes even down to the transition region [e.g., *Chertok and Grechnev*, 2003a; *Chertok et al.*, 2004a,b]. Evacuation of plasmas is possible if coronal structures are opened or stretched into the interplanetary space [*Delannée and Aulanier* 1999], which is proposed by CME models [e.g., *Antiochos et al.*, 1999; *Veselovsky and Panasenco*, 2002]. Direct evidence for plasma outflows has been provided by Doppler observations with Coronal Diagnostic Spectrometer on SOHO [*Harra and Sterling*, 2001]. Dissimilarities of some dimmings observed sometimes in different lines suggest that secondary temperature variations may also take place [*Chertok and Grechnev*, 2003b, *Chertok et al.*, 2004a], which can be also expected.

Another type of large-scale activity manifestations is represented by coronal waves that were first found from EIT images (often referred to as "EIT waves" for that reason). Such waves have been observed almost exclusively in the 195 Å channel because of the obvious reason: just this EIT channel is used for the imaging with a maximum rate of one full-disk image every 12 minutes in the standard CME Watch program. This rate is probably sufficient for detection of coronal waves, but not for their comprehensive study. Combining images produced in full-disk observations with the two telescopes, SPIRIT and EIT, provides better sampling of an event.

Observations and conceptions of coronal waves have been reviewed by *Zhukov and Auchère* [2004]. Some interpretations [e.g., *Delannée and Aulanier* 1999] connect propagation of the waves with phenomena of dimmings. Observations of coronal waves with TRACE in 171 and 195 Å almost simultaneously have been reported by *Wills-Davey and Thompson* [1999]. Observation of a coronal wave in soft X-rays with Yohkoh/SXT were discussed by *Khan and Aurass* [2002] and *Narukage et al.* [2002]. Recently, *Zhukov and Auchère* [2004] reported detection of coronal waves in the 284 Å band. No direct indications of strong temperature dependence for coronal waves have been found so far. Taking advantage of nearly simultaneous observations with the SPIRIT and EIT in close, but different bands of 175 and 195 Å, we also address this issue.

In this paper, we endeavor to make farther progress in understanding of these known, but still not well-understood phenomena, post-eruptive dimmings and coronal waves, and their probable relation to each other. In addition, we use the fact that, being shielded from energetic particles by the Earth magnetosphere due to the relatively low orbit of the CORONAS-F (altitude of 500 km), the SPIRIT supplies clean images when those acquired by the EIT are contaminated with "snowstorm" during/after proton events. This allows us analyzing those events in more detail.

2 Instrumentation

2.1 Telescopes and Observations

The SPIRIT complex was developed to study the solar activity in soft X-ray and EUV spectral bands. It contains two telescopes, the Ritchey–Chrétien telescope (171, 195, 284 and 304 Å bands), whose optics is identical to that of the SOHO/EIT telescope, and the Herschel two-band telescope with the 175 and 304 Å channels. In this paper, we discuss data obtained with the latter instrument. Because of a single reflection, its efficiency is higher in comparison with the Ritchey–Chrétien telescope, but its spectral band is wider. The spectral efficiency function of the 175 Å channel has a peak at 177 Å and a FWHM of 13 Å. Simulations with the CHIANTI code *Dere et al.* [1997] showed that this spectral range is optimal for observations of various solar features and phenomena from coronal holes to flares in the temperature band of $\log_{10} T(\mathrm{MK}) = 5.8 - 6.0$. The major part of the flux detected is due to bright spectral lines of FeIX–XI (excitation temperature $\log_{10} T = 5.9 - 6.1$) with lesser contribution of cooler OIV–V ($\log_{10} T = 4.6 - 5.4$) and hotter FeXX ($\log_{10} T = 6.9 - 7.5$) lines.

The 304 Å band of the Herschel telescope is peaked at 304 Å and has a FWHM of 46 Å. The major emission recorded in this channel contributes the transition-region HeII line (excitation temperature $\log T = 4.5 - 4.9$), but this band also includes intense lines of ions SiXI, FeXV, FeXVI, and FeXXIV excited at the temperatures of $\log_{10} T > 6$. The coronal and transition-region components can be separated using comparisons of simultaneous solar images in the 175 and 304 Å bands.

In the standard mode, the EIT produces full-disk heliograms every 12 minutes in the 195 Å band (CME Watch program), but only four times per day (every 6 hours near 01, 07, 13, and 19 UT) in 171, 284, and

304 Å bands. The SPIRIT recorded full-disk heliograms with time intervals between consecutive frames from 15 to 45 min in the 175 Å band during the first passage of the active complex (October 19–November 3), and in the 175 and 304 Å bands during its second passage (November 13–December 2). The SPIRIT observations are periodically interrupted by occultations (night times) of ~ 46 min in each of 15 orbits per day with an average period of ~ 94 min. Thus, simultaneous SPIRIT observations in 175 Å and 304 Å channels fill in 6-hour gaps in EIT observations in 171 and 304 Å bands.

It is well known that ideal instruments do not exist, each one has its own advantages and problems. In observations of powerful events, differences between the instrumental characteristics of the two telescopes clearly show up. Thus, combining observations with the two EUV telescopes, EIT and SPIRIT, we gain additional opportunities.

First, continuous observations carried out by the EIT in 195 Å channel with 12-min interval enables uniform coverage of the whole time interval of interest, without interruptions due to night time of a spacecraft flying in an orbit around the Earth. The EIT provides images of higher spatial resolution than the SPIRIT, but during strong flares they degrade from saturation effects, which interferes observations. On the other hand, observations with the SPIRIT do not show pronounced scattered light or saturation. Observations in close bands with two different telescopes simplify detection of instrumental contributions, when the features of interest appear dissimilar in their images.

Second, bright points and streaks, the so-called "snowstorm", supposedly due to energetic particles, are present in EIT images during/after proton events just after the flare maximum. However, this stage of an event is important for studies of the development of dimmings. The CORONAS-F/SPIRIT, being protected by the Earth magnetosphere against energetic particles, supplies clean images in those cases. Thus, the combination of both EIT and SPIRIT images gives a unique opportunity to observe a clear picture of flaring active regions and long-living dimmings for a long time.

2.2 Data Processing and Representation

Dimmings and coronal waves are relatively faint features. Hence, to detect them, differential methods are generally used. The whole area of a dimming can well exceed its appearance in non-subtracted images [see, e.g. *Zhukov and Auchère*, 2004]. This also means that studying dimming structures looking at an original image, without subtraction of a pre-event image, does not provide comprehensive information.

Following Paper I, we use fixed-base difference "derotated" images to study CME-associated disturbances. Such images are formed in two stages: first, the solar rotation is compensated for all images using three-dimensional rotation of the solar surface to the time of a base pre-event heliogram ("derotation"), and then the same reference heliogram is subtracted from all others. To reveal dimmings, which are faint, it is important to choose an appropriate brightness scale. We use a linear scale in a limited range of both positive and negative brightness. Such a technique allows us to form and analyze both SPIRIT and EIT fixed-base difference images in all available spectral bands with various time intervals, up to several hours.

On the contrary, running-difference images, which are formed by subtraction from each heliogram the preceding one, represent the temporal derivative of the image cube. They emphasize changes of the brightness, location, and structure of emitting features between two subsequent heliograms, which is useful, e.g., to detect coronal waves. However, this method is not suitable for studies of long-duration phenomena like dimmings. Therefore, we use in our study running-difference images as a helpful representation only.

The results of our analysis are illustrated below by several the most spectacular eruptive events of two rotations of the active regions. Additional images and movies for those and other events can be found at the Web site http://helios.izmiran.troitsk.ru/lars/Chertok/0310_11/spirit /index.html.

3 Events of the First Rotation

3.1 October 26

Two similar powerful eruptive events occurred on October 26: at first, at about 06 UT in the southern active region 486 (S15 E44), and then, at about 18 UT, in the western active region 484 (N02 W38). In this section, we consider the former event using the SPIRIT (175 Å) along with EIT (195 Å) observations. This event included a long-duration (LDE) 3B/X1.2 flare and a large CME of a partial-halo type with a bright loop front above the east limb.

The coronal wave in this event was observed with both EIT and SPIRIT as a faint, diffuse emitting structure at the interval from 06:21 to 06:46 UT. Panels (a–c) of Figure 1 show its positions at different times. Panel (e) shows the spatial profiles along the arrows computed by integration over the width indicated with the bars at

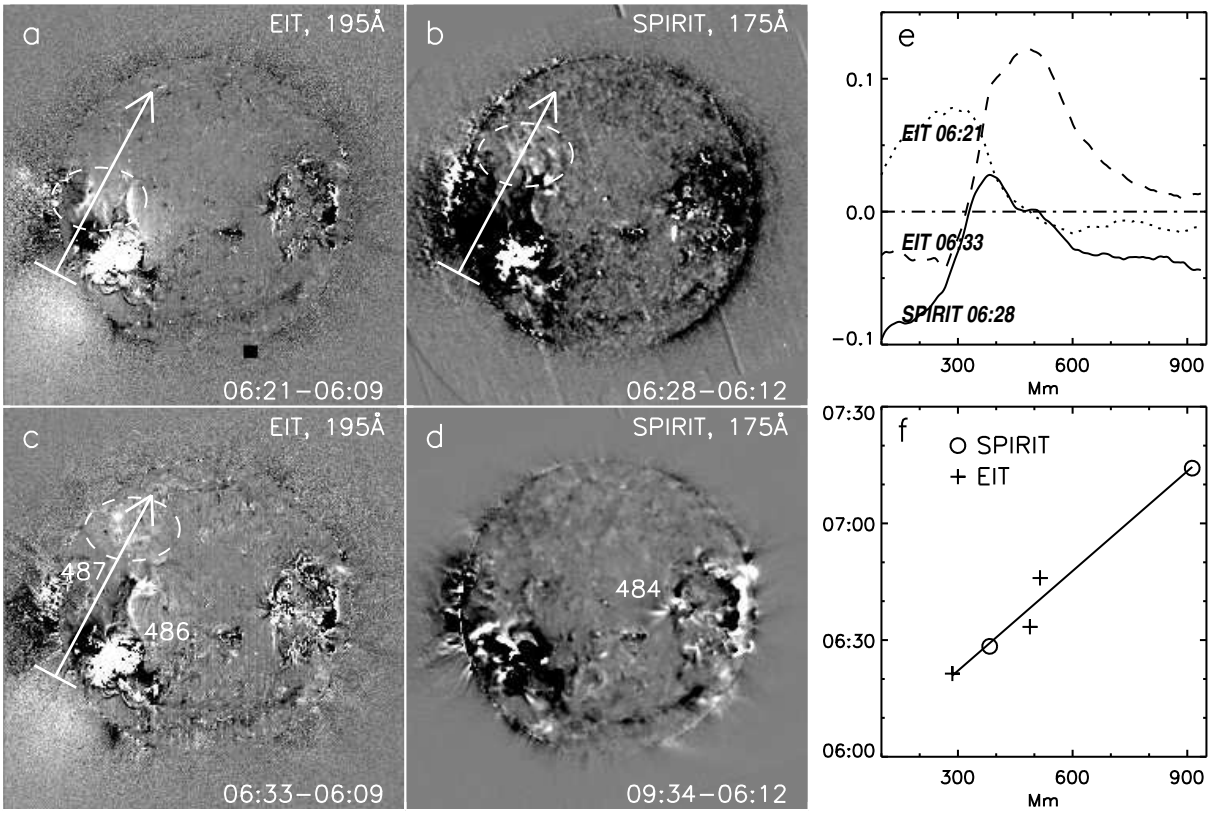

Figure 1: The October 26, 2003, 06 UT event in fixed-base difference "derotated" images observed with SPIRIT at 175 Å (b,d) and EIT at 195 Å (a,c) illustrating the coronal wave (marked with dashed ovals) and dimmings (dark areas). The arrows indicate approximate propagation direction of the wave. Panel (e) shows the profiles along the arrows obtained by the integration over the width indicated by the bars at the arrow bases. Panel (f) shows the positions of the profiles' peaks vs. time.

the arrow bases. The profiles are normalized to the pre-event images. Note that the brightness ranges in panels (b) and (d) are different according to the contrast of the wave and dimmings.

The positions of the wave in the images observed with the SPIRIT and EIT at different times correspond to the same moving feature (Figure 1f), although the wave is fainter in the 175 Å band. Combining the images produced with both telescopes, we estimate the speed of the wave of about 190 km s^{-1}. It propagates in a confined angular segment across the northeastern quadrant of the solar disk from the large southern active region 486 toward the northern polar area, passing by side of the AR 487. The area where the wave propagates does not contain active regions. Panel (d) shows that no dimming remains in this area after the pass of the wave.

The 12-minute cadence of EIT images at 195 Å is known to be insufficient for a detailed study of coronal waves, because in many cases they are visible in two to three frames only [e.g., *Biesecker et al.*, 2002]. In this respect, it is important that the SPIRIT 175 Å heliogram on October 26 was recorded at 06:28 UT, i.e., between two EIT 195 Å images at 06:21 and 06:33 UT. The combination of the EIT and SPIRIT observations provides more detailed information on the propagation of the coronal wave.

Already initial EIT and SPIRIT fixed-base difference derotated images in Figure 1a–d show that, besides the coronal wave, clearly visible dimmings (dark areas) appear around the eruption center in region 486. Moreover, starting from 06:21 UT, a very long and narrow arc-like lane dimming develops to connect the large active regions 486 and 484 disposed far from each other. It stretches through the high-latitude area of the southern hemisphere, becoming increasingly pronounced with time, and at the late phase of the event predominates in both SPIRIT 175 Å (Figure 1d) and EIT 195 Å images (not shown). This channeled dimming is clearly visible also in several preceding and subsequent eruptive events (see below and Paper I).

3.2 October 28

Outstanding global disturbances on the solar disk on October 28 were associated with the major eruptive event that occurred after 09:51 UT. A 4B flare took place in AR 486 (S16 E08). Its soft X-ray flux exceeded the

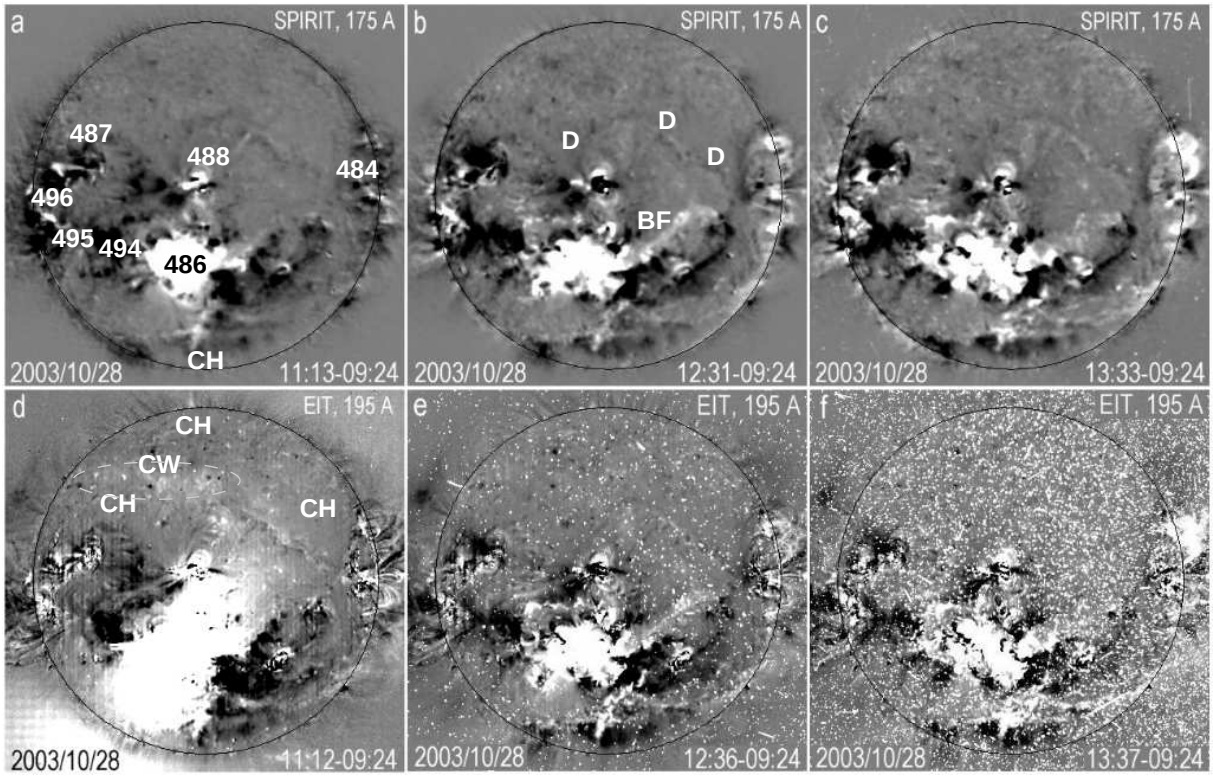

Figure 2: One of the most powerful, geo-effective event of October 28, 2003 as visible in SPIRIT 175 Å (a–c) and EIT 195 Å (d–f) fixed-base difference images for approximately the same times. The SPIRIT images are free of large-area saturation and diffuse scattered light as well of the "snowstorm" caused by energetic particles. Global dimmings extend mainly throughout the southern half of the disk and, a coronal wave (CW, marked with dashed oval) is observed with the EIT (d) in the northern hemisphere.

saturation level of the GOES monitors (X17.2) near 11:10 UT. An extremely high-speed ($V \approx 2400$ km/s) full-halo CME was observed in association with the event. This event also caused very strong proton fluxes and a severe geomagnetic storm ($D_{\rm st} \approx -363$ nT).

Figure 2 shows in the upper row (frames a–c) fixed-base difference derotated 175 Å SPIRIT images relative to the pre-event time of 09:24 UT. Analogous EIT 195 Å images are presented in frames d–f for approximately the same times. For this extremely intense event, that also produced powerful proton flux, the images acquired with EIT and SPIRIT differ. The first images after the eruption, in which dimmings are visible, were recorded by EIT at 11:12 UT (Figure 2d) and by the SPIRIT one minute later (Figure 2a). The dimming structure is difficult to see at that time, especially in the EIT image, because of very high brightness of the flaring region, which reached its maximum at 11:10 UT in both channels. A wide saturation area in the EIT image covers significant part of dimmings, and real intensities in its vicinity are distorted by the high level of scattered light. By contrast, the dimmings are visible in the SPIRIT image much better. The difference between SPIRIT and EIT images can be explained by several reasons. First, as model calculations using the CHIANTI database [http://wwwsolar.nrl.navy.mil/chianti.html] show, the flux for a medium flare in the 175 Å band is less than in the 195 Å band. Second, the signal in the SPIRIT detector does not reach full saturation, because of some non-linearity at high brightness levels. Third, the optical design of the SPIRIT telescope is based on one-mirror Herschel scheme with a large distance between the mirror and the detector. Hence, basically it has a lower level of scattered light than the shorter two-mirror Ritchey–Chrétien EIT telescope. In the next two images (not shown), both the SPIRIT and EIT display identical dimming structures, which look similar to those in Figure 2 (a,d). Thirty minutes after the flare maximum and later on, the dimming structure in the EIT images becomes indecipherable because of increasing number of bright points and streaks (the "snowstorm") due to energetic particles produced in the event. Only SPIRIT images can be used at this period to analyze dimmings. Thus, using the combination of images from both telescopes, we can comprehensively study this event.

The SPIRIT 175 Å fixed-base difference derotated images (a–c) demonstrate that dimmings cover almost the whole southern half of the solar disk and stretch between active regions. In particular, a narrow dimming connects the western neighborhood of the eruption center in AR 486 with the environment of AR 484 near the

west limb, in the same way as in the October 26 event. There is a trans-equatorial dimming connection between the eruption center and the northern region 488. The global picture of the disturbances throughout the whole southern hemisphere is emphasized with two bands of dimmings extending from two central active regions to the east limb, between AR 486 and 495 & 496 through AR 494, and between AR 488 and 487. A new "horizontal" dimming, located in the southern polar segment (perhaps near the boundary of the polar coronal hole), forms during this event. Just this dimming predominates in subsequent eruptive events (see Paper I and Section 3.4 of the present paper).

One more dimming (D), rather faint and extended, is detectable along the southeastern boundary of the western coronal hole in the northern hemisphere, which is obviously due to the decrease of brightness of a long chain of weakly emitting structures located there. The eastern end of this dimming is curved southward and comes finally to AR 488. The western end reaches the large active region 484, which is already close to the western limb. This faint dimming seems important in the context of the role of coronal holes in formation of dimmings [see, e.g., *Hudson and Webb*, 1997; *Thompson et al.*, 1998; *Zarro et al.*, 1999; *Gopalswamy and Thompson*, 2000; *Hudson and Cliver*, 2001, *Chertok and Grechnev* 2003].

Later on, the SPIRIT shows a dimming around AR 484 to evolve, likely due to an eruption in this region at about 12 UT. It occurs, probably, close to the limb or behind it. Signatures of the eruption are detectable in EUV images, but it has not been registered by the LASCO, likely due to strong contamination of images with "snowstorm". It is difficult to see this dimming in EIT images.

The EIT 195 Å image of 11:12 UT (Figure 2d) and, especially, the running-difference movie presented at the Web site specified in Section 2 show a faintly bright structure (CW). In this frame, it is localized in the northern hemisphere, nearly in parallel to the equator, and extends from the central meridian toward the eastern limb. This feature hardly can be due to the scattered light, which is definitely present in this image, because of its elongated shape and location, which are considerably different from the scattered light pattern, especially pronounced beyond the southeast limb. In a few subsequent frames, when looking at them in a narrow brightness range, one can reveal weak brightenings in a wide sector northward and toward the northeastern limb from its position in Figure 2d, while the faintly bright structure between the central meridian and the eastern limb disappears. These few frames show intermittent faint dark and bright features in a large area from this latitude up to the north pole. These properties correspond to a coronal wave, but it is difficult to determine its propagation direction, because the presence of coronal holes in that area complicates its appearance and motion. The scattered light in the EIT image does not permit us to judge about possible presence of the wave in the southern hemisphere. Like the wave in the event of October 26, it is faintly visible in 175 Å SPIRIT images, but still can be detected in careful examination. We do not present it here in detail, but only mention its properties: 1) the wave is detectable far from active regions, whereas dimmings are localized in active regions, in their vicinity, and between them (except for the dimming along the boundary of the southern polar coronal hole); 2) no pronounced long-living dimming follow the wave; 3) the wave is fainter in the 175 Å SPIRIT images than in the 195 Å EIT images.

Note also a bright feature (BF) that propagates over a very long distance from AR 486 northwestward. This fact also underlines the large-scale character of CME-associated disturbances.

3.3 October 29

On the next day, October 29, another very powerful and geo-effective event occurred in the same large superactive region AR 486 (S15 W02) from about 20:37 UT on. It was a 2B/X10 long-duration flare associated with a full-halo CME similar to that of October 28. The proton flux near the Earth also strongly enhanced in this case, and the accompanied severe geomagnetic storm achieved even greater value of $D_{\rm st} \approx -401$ nT.

The comparison of the SPIRIT 175 Å and EIT 195 Å fixed-base difference "derotated" images for this event (Figure 3) shows a similar picture. Again, we analyze the structure of dimmings based on SPIRIT images, because, like the previous day, EIT images are saturated and covered with strong "snowstorm". Nevertheless, one can conclude that SPIRIT and EIT images show very similar dimmings at 175 and 195 Å, especially several hours after the eruption.

The clean SPIRIT images (a,b) show that all dimmings are concentrated again in the southern hemisphere and the near-equatorial northern area. The interconnecting dimming observed in several preceding events between the eruption center in region 486 and the western region 484 is fragmentary. A conspicuous lane dimming along the northern boundary of the southern polar coronal hole, which initially formed one day before, becomes prevalent in this event, as well as a deep dimming going out of region 488 southeastwards. Besides, there are trans-equatorial dimmings between regions 486 and 488 and a double-branch dimming going from the same northern region 488 through region 487 to the eastern limb.

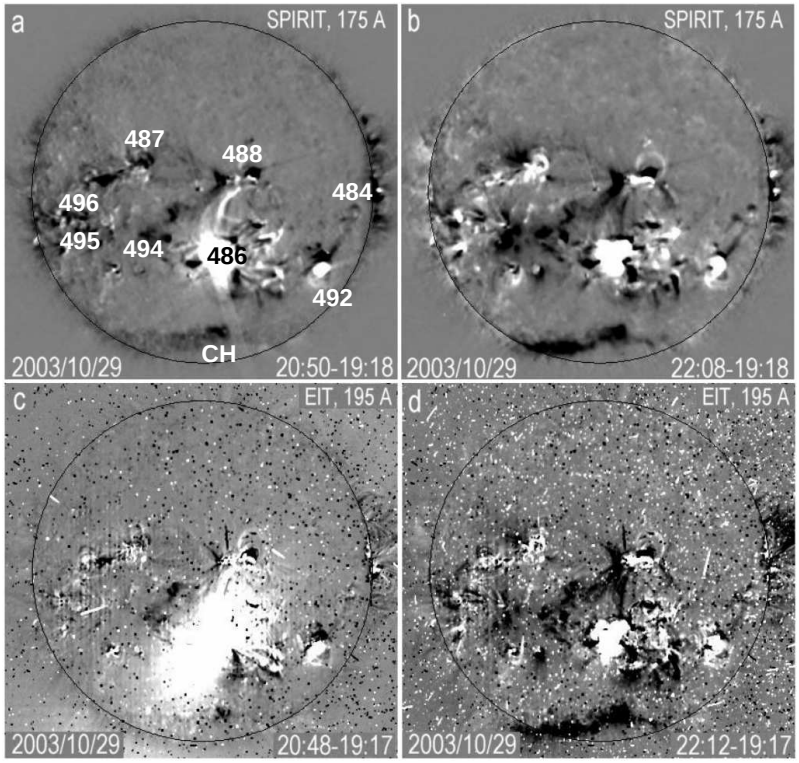

Figure 3: Comparison of SPIRIT 175 Å (a,b) and EIT 195 Å (c,d) fixed-base difference images for powerful event of October 29, 2003. Several large-scale channeled dimmings are better visible in cleaner SPIRIT images.

3.4 Large-scale Homology of Dimmings

Figure 4 summarizes common properties of six first-rotation events that occurred on October 23, 26, 28, 29, and November 2 as 175 Å difference SPIRIT post-eruptive images show. One can see that disturbances, which took place in those events, occurred in a huge activity complex constituted by three superactive large sunspot groups and some smaller active regions. Accordingly, a huge area was occupied by disturbances "highlighted" with dimmings that connected widespread active regions with each other (some of those connections being trans-equatorial), and even reached the southern polar region. The most prominent in events that occurred by October 28 was the arc-like lane structure *HD1*, which connected AR 484 and AR 486. The dimming structures obviously visualize the magnetic connectivity between the active regions.

Some dimmings observed in many recurrent eruptive events exhibit pronounced similarity in their shapes and locations (which is often referred to as their *homology*). Figure 4 shows that the arc-like lane structure *HD1*, which connected AR 484 and AR 486, dominated homologically by October 28. Previously, *Khan and Hudson* [2000] analyzed dimmings in trans-equatorial loops. *Chertok et al.* [2004a] reported homological large-scale dimmings and coronal waves for events in November 24–26, 2000 associated with one active region. By contrast, during the period of October–November 2003, a huge spatial area was embraced by repetitive dimming structures. Then, starting from October 28 on, this structure changed to another dominant configuration *HD2*, which was extended along the northern boundary of the southern polar coronal hole. This latter structure is visible in images of October 28, 29, and November 2 (Figure 4 d–f). As shown in Paper I based on EIT data, this polar dimming also dominated in the limb event of November 4 with the most powerful soft X-ray emission (this event was not recorded by the SPIRIT).

4 Events of the Second Rotation

The significant eruptive activity of the huge activity complex went on also when it was on the invisible side of the Sun, during November 6–12. Many large halo CMEs, which were recorded by LASCO without counterparts on the solar disk, certify this. The superactive regions 484, 486, and 488 appeared at the second rotation as ARs 501 (former 484; Carrington latitude and longitude N03, 002), 508 (former 486; S20, 286), and 507 (former 488; N10, 295). The eruptive events that occurred during the second pass of the activity complex across the

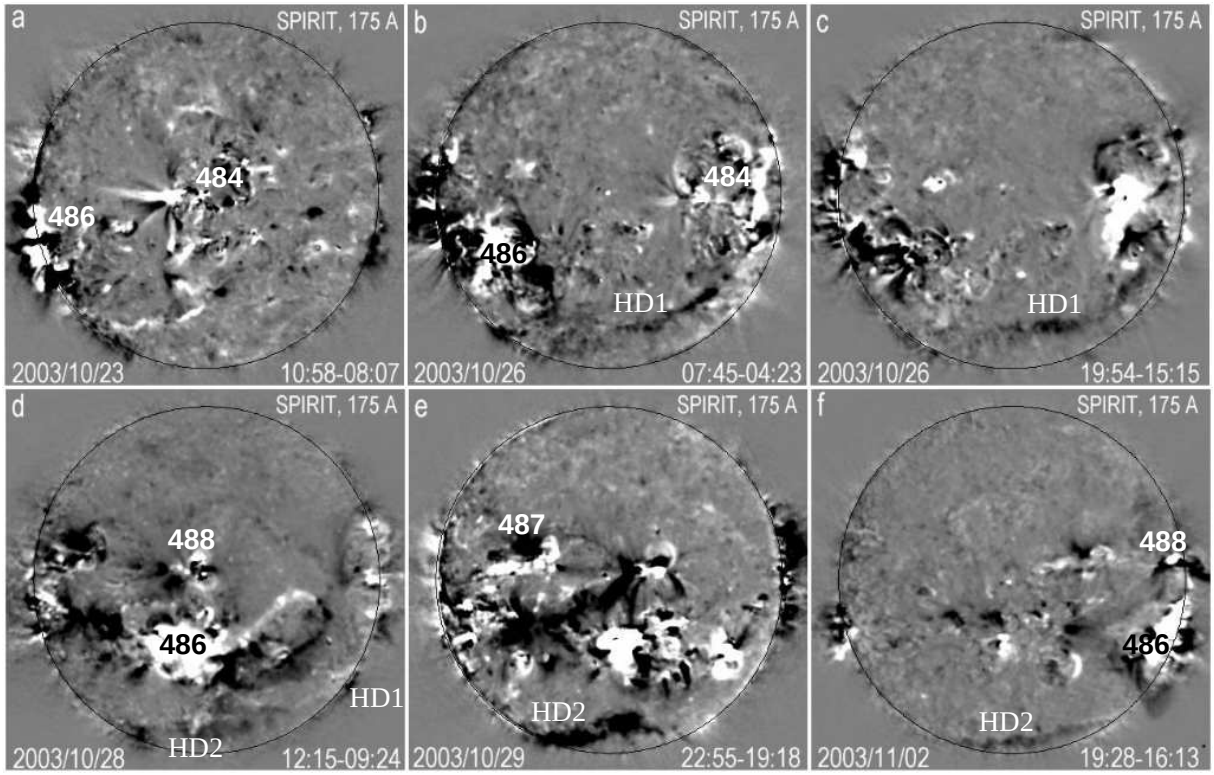

Figure 4: A collection of the SPIRIT 175 Å fixed-base difference images for several eruptive events observed during the first rotation of the activity complex illustrate homology of large-scale dimmings in the southern hemisphere. Before October 28(a–c), the arc-like lane structure *HD1* connecting AR 484 and AR 486 predominated. Starting from October 28 on, this structure changed to another dominant homological dimming *HD2* that extended along the northern boundary of the southern polar coronal hole.

solar disk were not as impressive as the first-rotation events; nevertheless, the activity was still high. The main dimming structure during the second rotation of the activity complex in November also embraced the southern half of the solar disk, as shown in Paper I. A series of geo-effective CME events occurred during November 17–18 in AR 501.

4.1 November 17

On November 17, a 1N/M4.2 flare occurred from 08:55 UT on, and a partial-halo CME was observed from 09:02 on. Figure 5 shows the fixed-base difference derotated images produced from heliograms of all four channels of the EIT (a, b, d, e), with images of 171, 284, and 304 Å being recorded with 6-hour intervals. It also shows images of two SPIRIT channels, 175 Å (c) and 304 Å (f). The SPIRIT 304 Å channel has a defect visible as a crack going from the right upper side of the frame toward the middle of the lower side. This defect is due to a fracture of the 304 Å filter that appeared in February 2003. It is wider in difference images, because the attitude of the spacecraft varies, thus resulting in apparent displacement of the solar image within the field of view.

The SPIRIT 175 & 304 Å and all EIT images show a deep long *L*-like dimming that originates from the southeastern side of the active region 501 and extends southward. This dimming is stable throughout the day. Some other dimmings adjoin the active region from the northwest and southwest. A compact dimming is also observed in region 503. The major *L*-like dimming coincides in all coronal lines, and it is manifest in the transition-region 304 Å band in both EIT and SPIRIT images. It is more pronounced in the SPIRIT than in the EIT 304 Å image, likely due to wider spectral response of this SPIRIT channel and larger contribution of hotter coronal lines in its 304 Å band.

4.2 November 18

This event was observed as a 2N optical LDE flare in AR 501 (N08 E18) with two X-ray bursts of M3.2 (07:52 UT) and M3.9 (08:31 UT). The first flare event was probably related to disappearance of a large horseshoe-shaped

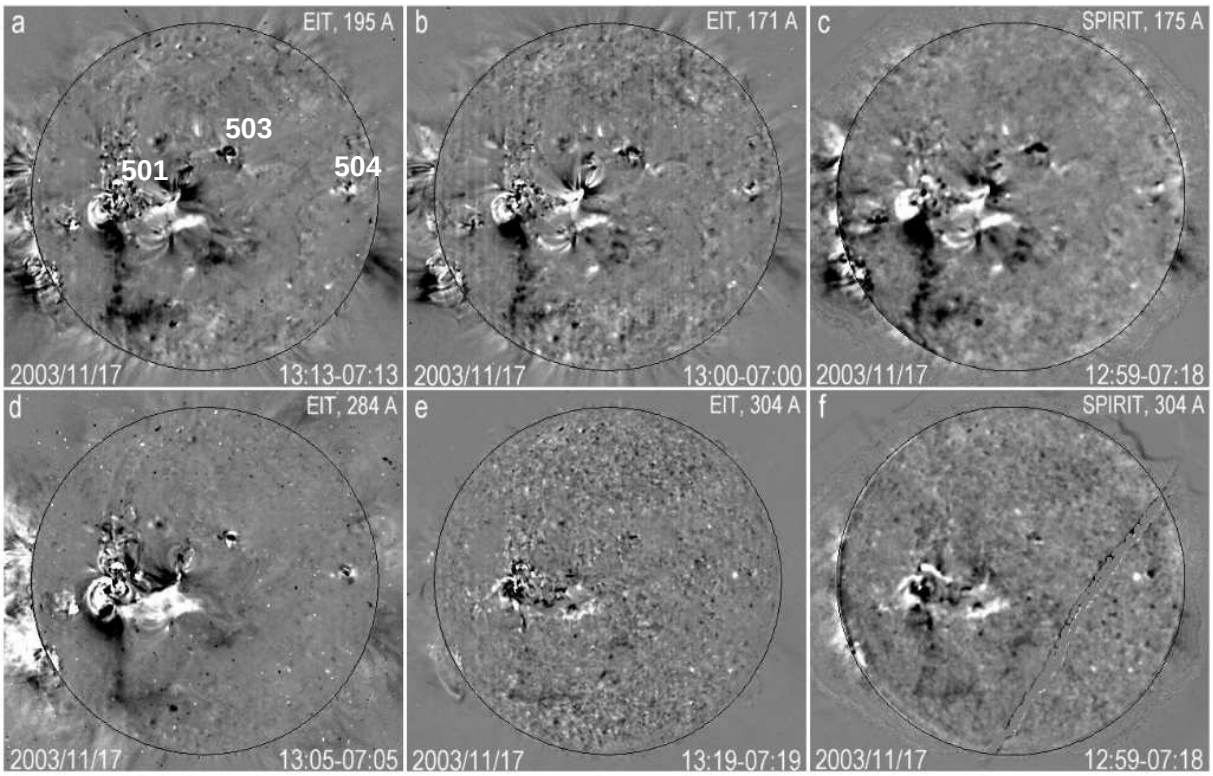

Figure 5: Fixed-base difference images of the November 17, 2003 event observed with 6-hour intervals in all four EIT bands of 195, 171, 284, 304 Å (a,b,d,e) and in the SPIRIT 175 and 304 Å bands (a,b). The major southern dimming coincides in all coronal lines, and manifests itself in a similar way in the transition-region 304 Å line in both EIT and SPIRIT images.

filament, which was localized southwestward of AR 501. This occurred between 07:43 and 07:48 UT, according to Hα observations at the Kanzelhöhe Solar Observatory. The third, additional M4.5 X-ray burst with a maximum at 10:11 was due to some activity at the western limb. The corresponding CME also had several components. Initially, a relatively weak CME was observed above the southeastern limb with the brightest western portion of the front, like the CME of November 17. Next, after about 08:50 UT, much brighter, rapid ($\simeq 1650\,\mathrm{km\,s^{-1}}$), large-scale partial-halo CME appeared above the southern and southwestern limb (the central position angle about 214°, and the start time, which we extrapolate in the sky plane to the position of AR 501, is 07:59 UT). Despite the moderate flare importance, just this event caused the most powerful geomagnetic storm with $D_{\mathrm{st}} \approx -465$ nT on November 20. The third large CME, observed above the southeastern limb from 09:26 UT on, was likely due to some activity in adjoining sector of the invisible hemisphere. EIT and SPIRIT images (Figure 6) also show it just above the limb. Note that fifteen SPIRIT 304 Å heliograms supplement two corresponding EIT images observed at 07:19 and 13:19 UT on that day.

The CME of 08:50 UT was accompanied by significant disturbances also over almost the whole southern portion of the disk. Both EIT and SPIRIT images show development of deep dimming structures that surround the eruption center from the south and west and extend toward the southwest limb. The major dimmings around the AR 501 are almost at the same places as one day before, with two exceptions: a new dimming appears southwestward of the active region, but the southwestern branch (the base of the "L"), which was observed on the previous day, is absent. The most remarkable is the conspicuous, almost straight, lane dimming extended southeastward, which shows a great deal of similarity in its shape and position with the dimming on the previous day. All the dimmings coincide in the coronal channels of EIT, 195 Å (a–c), and SPIRIT, 175 Å (d–f), with some their parts being also pronounced in the SPIRIT 304 Å (g–i) band.

Simultaneously, westward of the straight lane dimming, the coronal bands show for some tens of minutes a complex system of disturbances, both standing and propagating from the eruption center. In particular, a coronal wave (CW) is observed at 08:00–08:48 UT to propagate from the eruption center southward in the 195 Å EIT and 175 Å SPIRIT bands. It is also detectable in the 304 Å SPIRIT band, but much weaker. Probably, this is due to hotter coronal lines present in this band. Note that extended dimmings in the southwestern area cease after 10:00 UT.

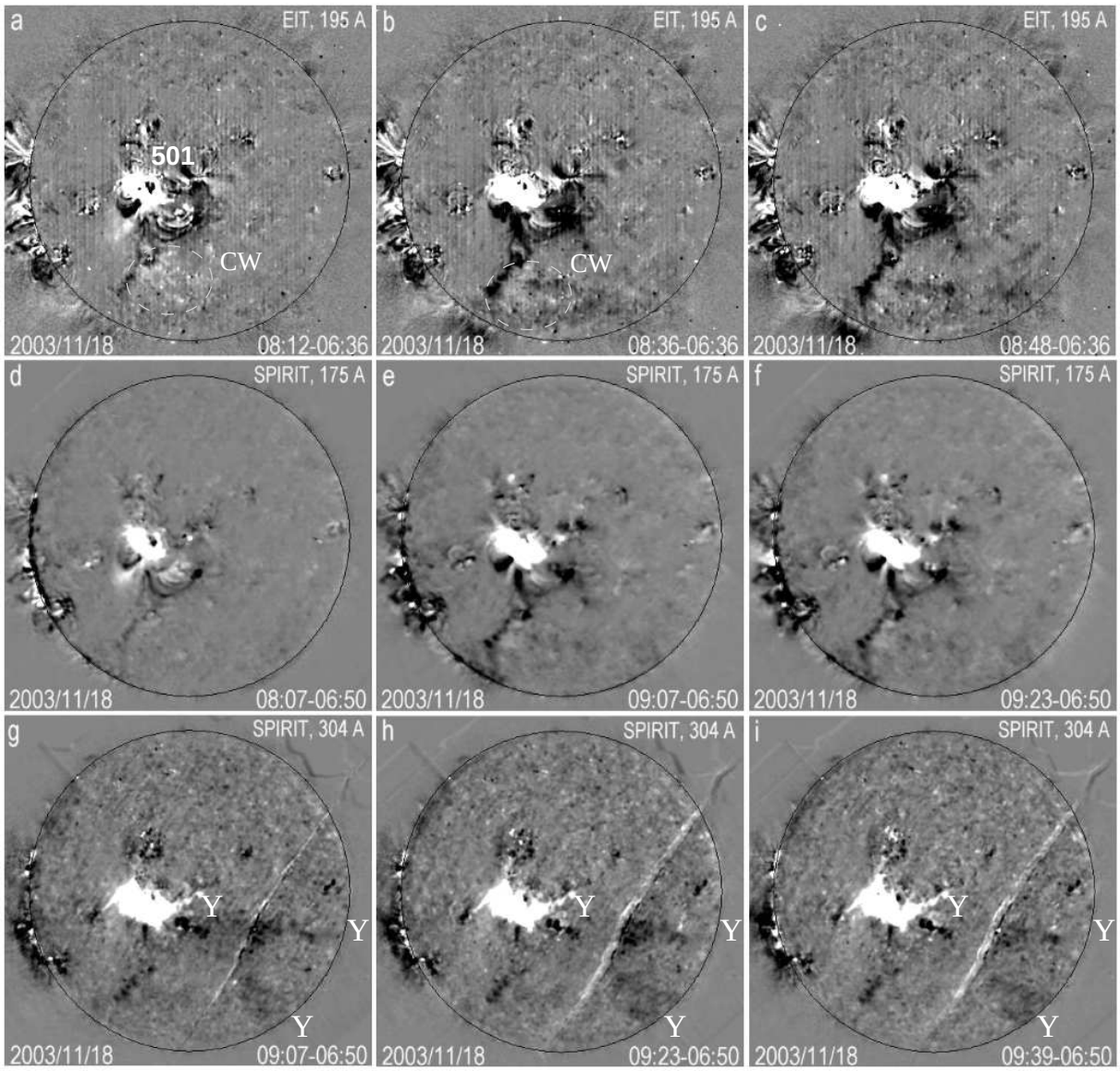

Figure 6: Fixed-base difference images of November 18, 2003 event: large-scale disturbances observed with EIT at 195 Å (a–c) and with SPIRIT at 171 Å (d–f) & 304 Å (g–i). The major southern dimming looks similar in all three bands. The coronal wave (CW) is marked in frames (a,b) with dashed ovals. The SPIRIT 304 Å images (g–i), recorded with a relatively good time coverage, display a "Y"-like dark feature (marked with "Y" at its vertices) propagating from the eruption center in AR 501 to the southwestern limb.

The 304 Å SPIRIT images show detectable transition-region analogs of the main coronal dimmings. In addition, the 304 Å heliograms (Figure 6g–i) clearly show from 08:23 to 09:54 UT a dark "Y"-like feature to propagate from the eruption center toward the southwest limb. It appears when the leading edge of the CME reaches the distance of $2.6R_{\odot}$. The sky-plane propagation velocity of this dark feature is about $150\,\mathrm{km\,s^{-1}}$. At 10:43 UT, it fully disappears at the disk, and no manifestations of this feature related the CME of 08:50 UT are visible above the limb. This feature with a maximum depth of up to −30% was observed at the 304 Å channel, but it was not revealed in the coronal bands. This propagating feature lags behind the coronal wave observed in the 195 and 175 Å bands by several tens of minutes (see the movie at the Web site referred to in Section 2).

5 Discussion

Taking advantage of the combined observations with the two EUV telescopes, we can overview large-scale activity manifestations during October–November 2003. Generally, dimmings are well pronounced and similar in moderate-temperature coronal lines, 171 and 195 Å observed with EIT, and 175 Å observed with SPIRIT. Some dimmings are also detectable in the 304 Å band, especially, near the eruption center. Note that this band includes not only the cool transition-region line of HeII (0.05–0.08 MK), but it also catches a small part of hotter coronal lines. The hotter contribution is probably more distinct for the SPIRIT EUV telescope due to wider spectral response, which can be seen for some events from the comparison with the 175 Å images.

5.1 Dimmings: Global Disturbances and Homology

From the fixed-based difference images that we have presented, one can see that manifestations of large-scale disturbances in all events embraced the entire southern half of the solar disk and mainly extended between three large superactive regions, disposed far from each other (see Figure 4). This was especially pronounced in the major event of October 28 (see Figure 2). No manifestations of deep, long-term dimmings were visible at the northern hemisphere, at latitudes above those of active regions. Mid-latitude extended coronal holes were present there, which obviously affected the dimmings (e.g., the faint elongated dimming in the October 28 event, Figure 2). First, to observe something to dim, some pre-event emission must be present, but it is weak in coronal hole regions. Second, coronal holes are known to be regions of open magnetic fields, hence, the conditions for CME-associated disturbances to develop within them are different from those outside coronal holes. These two reasons can account for the absence of deep, long-living dimmings in the northern hemisphere.

The dimming structures seen in the 175 Å band practically coincide with those observed in the 195 Å band. They are less pronounced at 304 Å. Nevertheless, the presence of detectable dimmings in the 304 Å band shows that perturbations responsible for dimmings after eruptive events took place not only in the corona, but they also involved the transition region. We note herewith that the SPIRIT observed the development of dimmings in the 304 Å band in another major event (November 4, 2001) to lag behind coronal dimmings visible at the 175 and 284 Å by at least half an hour [*Chertok et al.* 2004b]. This fact confirms gradual evolution of dimmings from the corona down to the transition region, and it is important in understanding the development of the eruption process and evolution of magnetic structures.

As shown in Paper I, the main dimming structures in recurring events of October 2003 were homological. Homology of large-scale dimmings in a series of events probably traces some large-scale connections in the corona. These connections may not be well pronounced in a particular event, but their repetitive appearance, even fragmentary or patchy, reveals this large-scale connectivity. Homology of dimmings shows that large-scale magnetic configurations (with a spatial scale of order of the extent of the activity complex) were relatively stable. This also means that the large-scale emitting structures, which exhibited homology, restored their brightness between sequential eruptions, at least, partly.

The dimming structures in repetitive events did not always perfectly coincide. This seems reasonable also, because some changes may take place in the large-scale magnetic configuration between the sequential eruptive events. We also see that the change occurred on October 28 from one large-scale homological structure, arc-like lane between AR 484 and AR 486, to another structure, nearly along the boundary of the southern polar coronal hole.

The fact that dimmings are widespread over a huge area with a spatial extent comparable with the solar radius or even diameter confirms the non-local nature of the CME process. However, results of eruptions are not uniform among the totality of dimmings and other large-scale disturbances observed. Dimmings are often pronounced in those regions, which were conspicuously bright before the eruption, but this is not true generally [see, e.g., *Chertok and Grechnev*, 2003a]. So, the picture of dimmings does not reproduce the inverted pre-event image. So, with the global character of CME-associated disturbances, they are manifest not equally in different

structures involved. In the context of the idea that dimmings show "the coronal signatures (i.e., remnants) of magnetic flux ropes ejected during CMEs" (or CME's "footpoints") [see, e.g., *Hudson and Webb*, 1997; *Zarro et al.* 1999; *Webb et al.* 2000] this means that the real situation is more complex. This interpretation can work for compact twin dimmings near post-eruptive arcades, but the structure of a real CME, whose eruption involves a huge activity complex, is definitely more complex than a simple single flux rope.

5.2 Coronal Waves

Coronal waves were observed during events of October 26 (see Figure 1) and November 18 (see Figure 6). On October 26, it is pronounced in both 175 Å SPIRIT and 195 Å EIT channels. We have shown here the fixed-base difference images to reveal dimmings, but the running-difference those could emphasize the waves with a higher contrast. The sky-plane propagation speed of the coronal wave on October 26 estimated from the combination of images produced with both telescopes is of order 190 km/s for its central part, which seems to be an ordinary velocity for a coronal wave [*Thompson et al.*, 1998, 1999].

On October 28, a relatively bright, diffuse structure with properties of a coronal wave is visible in EIT image of 11:12 UT. It is also detectable in 175 Å SPIRIT movie, thus confirming the reality of the phenomenon, but it is faint in this band again. Similar situation was for the observation of the coronal wave on November 18. In all the three cases, coronal waves look less pronounced in the 175 Å SPIRIT images than in the 195 Å EIT those. The temperature ranges for the FeIX–XI 175 Å and FeXII 195 Å lines are rather close, with the temperature sensitivity maximum being narrower and slightly displaced to lower temperatures in the 175 Å SPIRIT band. On the other hand, the 195 Å EIT band has wider low-sensitivity wings toward both lower and higher temperatures. These facts hint that the different brightness of the coronal waves in these two bands can be due to emission of hotter plasmas that are probably present, to which the 195 Å EIT band is more sensitive.

Note that some existing impressions on dimmings acquired from analyses of running-difference images may not be correct. For example, moving "dimmings" just behind coronal waves in running-difference images sometimes can be nothing but a differentiation effect. *Zhukov and Auchère* [2004] proposed a bimodality of coronal waves, with the "wave mode" being a classical (MHD) wave, and the "eruptive mode" being due to the emission of material erupted. In particular, when dealing with a wave-like process, one might expect short-term alternate bright and dark features, which then disappear. In this respect, we note that in all three events considered, long-term, deep dimmings did not follow coronal waves, especially when the latter were observed far from the eruption centers. The disturbances, both coronal waves (when observed) and dimmings, affected the whole visible solar surface, but the coronal waves were mainly observed in those areas, where no active regions were present, whereas dimmings were manifest mainly in active regions, in their vicinity, and between them. Coronal waves are generally known to avoid active regions and not to enter coronal holes [*Ofman and Thompson*, 2002]. All these facts are incompatible with a common interpretation of coronal waves as a propagating boundary of a dimming [see, e.g., *Delannée and Aulanier*, 1999, *Delannée*, 2000]. So, the relation of these phenomena does not seem to be straightforward generally. If there is a real connection between them, then it occurs a more complicated fashion.

5.3 Moving Dark Feature in November 18 Event

Panels g–i of Figure 6 illustrate a remarkable moving dark feature that was observed on November 18, between 08:23 and 09:54 UT in the SPIRIT HeII 304 Å band. Previously, some dark features were observed with EIT in the 304 Å band without counterparts in coronal lines [*Delaboudinière*, private communication; *Chertok and Grechnev*, 2003b], but in single frames only and without simultaneous observations in other bands. Therefore, it was not possible to analyze their properties and behavior.

This feature cannot be interpreted in terms of plasma outflow, because it was not observed in coronal bands. This phenomenon rather could be produced by some moving opaque material. Absorption of this material diminished the solar disk emission by about 30% at 304 Å, but it was much less at both 175 and 195 Å. The fact that this feature was not observed at 175 Å suggests that the temperature of its material was lower than the coronal one. In principle, two absorption mechanisms could respond for this phenomenon: 1) resonant absorption at HeII 304 Å line, if the temperature of this feature does not exceed 0.08 MK, or 2) non-resonant absorption, mainly, in neutral hydrogen, if the dominant temperature is quite low, of order 5000 K. We cannot rule out either of these absorption mechanisms. Therefore, we can only state that the temperature and density of the absorbing material were rather low; otherwise, we would observe manifestations of absorption at 175 Å.

As we noted, a horseshoe-shaped filament was ejected from AR 501 at about the time of the eruptive event onset. The location of the eruption center, N00 E18, and the configuration of the relevant CME (nearly halo with a central position angle of about 214°) show that the eruption direction was conspicuously non-radial, with a

pronounced southwestern tendency. This corresponds to the motion direction of the absorbing feature (just the orientation of its southwestern branch). Therefore, the absorbing material could be a "cloud" formed from the material of the filament ejected earthward-southwestward, which probably failed to become a core of the same CME. This is confirmed with the closeness of extrapolated launch times of this cloud (about 07:52 UT), CME (07:59 UT), and the filament (07:43–07:48 UT).

Figure 6g–i and the corresponding movies show that the by-limb portion of the dark propagating feature was almost stationary, whereas another part observed just to the left of the fracture showed pronounced motion southwestward, toward the solar limb. From these facts we conclude that the moving dark feature consisted schematically of two components, with one fallen down on the solar surface close to the limb, and another one, which flew over a longer distance and, probably, fell down behind the limb.

All the facts can be reconciled if we suppose some absorption to take place in the remnants of the eruptive filament, with planes of their trajectories being close to the line of sight, forming something like a spray (or two sprays). The fact that the filament remnants had not appeared outside the limb (probably, fell down on the solar surface) consists with absence of a pronounced core in the large halo CME associated with this eruption (the first appearance at 08:50 UT). It is not clear, however, whether absence of the core in the CME had any relation to its rather high speed (about 1650 km/s).

In this connection, we note that not all darkening effects can only be interpreted in terms of the density depletion. We already mentioned propagating dark features sometimes observed to accompany coronal waves. Short-term and moving dark features, especially those observed in the 304 Å band only without counterparts in coronal lines, definitely suggest some occultation of the emission from underlying plasmas by absorbing material of ejecta, i.e., eruptive filament or its remnants. EIT observations at 195 Å also show many examples of occultation phenomena [see, e.g., *Uralov et al.*, 2002]. A convincing example of an occultation effect without any detectable manifestations at coronal bands is presented by the event of November 18, when such moving dark feature was observed with the SPIRIT in the 304 Å band only.

5.4 Particle Traces in Images

Bright points and streaks in EIT (and LASCO) images called also the "snowstorm" are supposed to be due to impacts of energetic particles (and secondary particles produced by them) reaching the CCD matrix of the telescope [see, e.g., *Andrews* 2001]. The major contribution to the "snowstorm" is likely due to protons with energies of some tens of MeV. This follows, in particular, from the fact that the "snowstorm" usually starts tens of minutes after the assumed ejection time of particles from the flare site. Furthermore, *Grechnev* [2004] showed that the time profiles of the snowstorm density in EIT images highly correlate with 40–80 MeV proton flux recorded near the Earth by GOES. So, just those protons (and/or secondary particles produced by them) are mainly responsible for the snowstorm effect in EIT images. During proton events of October 28 and 29, we see that, as the proton flux increases, snowstorm from energetic particles covers the EIT images increasingly, but no snowstorm is present in SPIRIT images. The reason is that the SOHO is located 1.5 million km sunward of the Earth in the *L1* Lagrangian point, i.e. far outside of the Earth magnetosphere. Such a location is very suitable for continuous observations of the Sun, but the telescope is exposed there to strong proton fluxes. Note herewith that snowstorm in EIT images becomes strong when the proton flux with $E > 10$ MeV exceeds some hundreds particles/(cm^2 s sr).

On the other hand, the CORONAS-F satellite flies in a low orbit at about 500 km around the Earth. Therefore, observations of the Sun with SPIRIT have interruptions due to the night times of the spacecraft, but its images are free of snowstorms (which confirms again that they are produced by charged particles). The magnetosphere of the Earth deflects energetic particles, thus shielding the SPIRIT. Hence, SPIRIT images provide us with clearer picture of CME-associated disturbances on the solar disk even under the presence of strong proton fluxes.

6 Summary and Concluding Remarks

We have studied CME-associated large-scale manifestations on the solar disk during the extraordinary outburst of the eruptive solar activity in October and November 2003 using observations with two EUV telescopes, CORONAS-F/SPIRIT at 175 and 304 Å and SOHO/EIT at 195 Å, which essentially complement each other both in temporal and spectral coverage. We have addressed post-eruptive dimmings and coronal waves in major events of that period. Observations of long-term dimmings are important for studies of the dynamics of large-scale magnetic structures. In particular, we have found that most dimmings appeared in active regions, in their vicinity, and between them, thus highlighting the large-scale magnetic connectivity. In turn, it shows that CME-associated disturbances occurred in a single, huge, interconnected activity complex consisting of three large

superactive regions 484 (501), 486 (508), 488 (507) and smaller active regions. This complex produced several extremely powerful events during its presence on the visible side of the Sun at the first rotation, and then the activity decreased at the second rotation, but still was very high.

The CME-associated large-scale manifestations during that period embraced a huge area of the visible solar surface. Our analysis has shown that dimmings, having once appeared, then existed for many hours. They were most pronounced in the southern part of the visible solar disk, where the major part of the activity complex was localized. Nearly simultaneous observations in 304, 175, and 195 Å bands showed that dimmings formed both in the corona and the transition region being similar in shapes and sizes. This supports the assumption of their origination due to density depletion.

We have found homology of some dimming structures in recurring events that occurred by October 28. It changed to another homological structure on that day, which persisted in later events. Homology of large-scale dimmings in a series of events probably traces some large-scale connections in the corona. They may not be well pronounced in a particular event, but their repetitive appearance, even fragmentary or patchy, reveals them. Homology of dimmings shows that large-scale magnetic configurations (with a spatial scale of order of the extent of the activity complex) were relatively stable. Possibly, in some cases they can restore the brightness of emitting arch structures. All these facts are suggestive of the global character of CME-associated disturbances, which seems important in considerations of CME models.

Being shielded by the Earth magnetosphere, SPIRIT images do not suffer from particle traces during severe proton events. Using this fact, we have followed the development of a large dimming between the active regions 484 and 486 on October 28 after 12 UT, which was not visible in EIT images. Moreover, this fact suggests a coronal mass ejection from that region, which also could not be detected by the LASCO due to the strong "snowstorm".

We have analyzed the first nearly simultaneous observations of coronal waves in two bands, 175 and 195 Å, and shown that the waves look fainter in the 175 Å band. This suggests contribution of hotter-plasmas emission. Our analysis of coronal waves observed in some events, in particular, far from the eruption centers, and deep, long-living dimmings has shown that they took place mainly in different parts of the solar surface. This means that generally these phenomena are not directly related, and this is incompatible with the idea about coronal waves as a propagating boundary of a dimming of that kind for those events.

Taking advantage of simultaneous SPIRIT observations at 175 and 304 Å with sufficient imaging rate, on November 18 we observed for the first time a dark moving ejecta across the solar disk in the 304 Å band without counterparts in coronal lines. We interpret this observation as a "cloud" formed from material of the eruptive filament, which probably failed to become a CME core.

Our results show opportunities of simultaneous observations of solar phenomena in close bands with two similar space telescopes, CORONAS-F/SPIRIT and SOHO/EIT, whose orbits and operating conditions are different. Both similarity and difference of the phenomena observed clearly show up in combined images and movies formed from the images acquired with those telescopes. In particular, the overall similarity of dimmings (as well as other phenomena) observed at 175 and 195 Å provides a possibility to study their development during many hours using SPIRIT data when strong flare emissions and/or severe proton fluxes are present in EIT images. Combining images produced with these telescopes, it is possible to study the movement of coronal waves with better temporal coverage. In summary, using such combinations, one can study the whole story of an event, including flare maximum and late post-eruptive manifestations. Some movies illustrating these opportunities are presented at the Web sited mentioned in Section 2.

Acknowledgments. We are grateful to Acad. I.I. Sobelman and Prof. V.D. Kuznetsov, scientific leaders of the CORONAS-F project, for the interest and support of this study; A. N. Zhukov for fruitful discussions; and the CORONAS-F team in IZMIRAN for their assistance in the telemetry data supply. We thank the referees, I.S. Veselovsky and the anonymous referee, for useful comments. We are grateful to SOHO/EIT team members for data used in this research, and to the Kanzelhöhe Solar Observatory, whose Hα images helped us, too. We also used the CME catalog generated and maintained by NASA and the Catholic University of America in cooperation with the Naval Research Laboratory. SOHO is a project of international cooperation between ESA and NASA. This work is supported by the Russian Foundation of Basic Research (grants 02-02-17272, 03-02-16049, 03-02-16591), the Federal Ministry of Education and Science (grants NSh 447.2003.2, 1445.2003.2), and the Program No. 16 of the General Physics Department of RAS.

References

Andrews, M. D. (2001), LASCO and EIT observations of the Bastille Day 2000 solar storm, *Solar Phys.*, *204*, 181–198.

Antiochos, S. K.; C. R. DeVore, J. A. Klimchuk (1999), A model for solar coronal mass ejections (1999), *Astrophys. J.*, *510*, 485–493.

Biesecker, D. A., D. C. Myers, B.J. Thompson et al. (2002), Solar Phenomena Associated with "EIT Waves", *Astrophys. J.*, *569*, 1009–1015.

Chertok, I. M. and V. V. Grechnev (2003a), Solar large-scale channeled dimmings produced by coronal mass ejections, *Astron. Reports*, *47*(2), 139–150.

Chertok, I. M. and V. V. Grechnev (2003b), Large-scale dimmings caused by coronal mass ejections at the Sun according to SOHO/EIT data in four EUV lines, *Astron. Reports*, *47*(11), 934–945.

Chertok, I. M., V. V. Grechnev, H. S. Hudson, and N. V. Nitta (2004a), Homologous large-scale activity in solar eruptive events of 24–26 November 2000, *J. Geophys. Res.*, *109*, A02112, doi:10.1029/2003JA010182.

Chertok, I. M., V. A. Slemzin, S. V. Kuzin, V. V. Grechnev, O. I. Bugaenko, I. A. Zhitnik, A. P. Ignat'ev, and A. A. Pertsov (2004b), Analysis of a solar eruptive event on November 4, 2001, using CORONAS-F/SPIRIT data, *Astron. Reports*, *48*(5), 407–417.

Chertok, I. M., and V. V. Grechnev (2005), Large-scale activity in solar eruptive events of October–November 2003 observed from SOHO/EIT data, *Astron. Reports*, *49*(2), 155–166 (Paper I).

Delaboudinière, G.-P., E. Artzner, J. Brunaud et al. (1995), EIT: Extreme-Ultraviolet Imaging Telescope for the SOHO Mission, *Solar Phys.*, *162*, 291–312.

Delannée, C. (2000), Another view of the EIT wave phenomenon, Astrophys. J., *545*, 512–523.

Delannée, C. and G. Aulanier (1999), CME associated with transequatorial loops and a bald patch flare. *Solar Phys.*, *190*, 107–129.

Dere, K. P., E. Landi, H. E. Mason, B. C. Monsignori Fossi, P. R. Young (1997), CHIANTI – an atomic database for emission lines, *Astron. Astrophys. Suppl. Ser.*, *125*, 149–173.

Dere, K. P.; J. D.Moses, J.-P. Delaboudinière, J. Brunaud, C. Carabetian, J.-F. Hochedez et al. (2000), The Preflight Photometric Calibration of the Extreme-Ultraviolet Imaging Telescope EIT, *Solar Phys.*, *195*, 13–44.

Grechnev, V. V. (2004), Solar Energetic Particles in SOHO/EIT images: cleaning images and particle diagnostics, in *Multi-Wavelength Investigations of Solar Activity*, Proc. IAU Symp. 223, 2004, edited by A.V. Stepanov, E.E. Benevolenskaya, and A.G. Kosovichev, International Astronomical Union, 625–626.

Gopalswamy, N. and B. J. Thompson (2000), Early life of coronal mass ejections, *J. Atmos. Sol. Terr. Phys.*, *62*, 1457–1469.

Harra, L. K. and A. C. Sterling (2001), Material Outflows from Coronal Intensity "Dimming Regions" during Coronal Mass Ejection Onset, *Astrophys. J.*, *561*, L215–L218.

Harrison, R. A., P. Bryans, G. M. Simnett, and M. Lyons (2003), Coronal dimming and the coronal mass ejection onset, *Astron. Astrophys.*, *400*, 1071–1083.

Hudson, H. S. and D. F. Webb (1997), Soft X-ray signatures of coronal mass ejections, *Geophysical Monographs*, *99*, 27–38.

Hudson, H. S. and E. W. Cliver (2001), Observing CMEs without coronagraphs, *J. Geophys. Res.*, *106*, 25199–25214.

Khan, J. I. and H. Aurass (2002), X-ray observations of a large-scale solar coronal shock wave, *Astron. Astrophys.*, *383*, 1018–1031.

Khan, J. I. and H. S. Hudson (2000), Homologous sudden disappearances of transequatorial interconnecting loops in the solar corona, *Geophys. Res. Lett*, *27*(8), 1083.

Narukage, N., H. S. Hudson, T. Morimoto et al. (2002), Simultaneous Observation of a Moreton Wave on 1997 November 3 in Halpha and Soft X-Rays, *Astrophys. J.*, *520*, L139–L142.

Ofman L. and B.J. Thompson (2002), Interaction of EIT Waves with Coronal Active Regions. *Astrophys. J.*, *574*, 440–452.

Oraevsky, V. N. and I. I. Sobelman (2002), Comprehensive Studies of Solar Activity on the CORONAS-F Satellite *Astron. Letters*, *28*, 401–410.

Oraevsky, V. N., I. I. Sobelman, I. A. Zitnik et al. (2003) CORONAS-F observations of active phenomena on the sun, *Adv. Space Research*, *32*(12), 2567–2572.

Thompson, B. J., S. P. Plunkett, J. B. Gurman et al. (1998), SOHO/EIT observations of an Earth-directed coronal mass ejections on May 12, 1997, *Geophys. Res. Lett.*, *25*, 2465–2468.

Thompson, B. J., J. B. Gurman, W. M. Neupert et al. (1999), ApJ, 517, L151 SOHO/EIT Observations of the 1997 April 7 Coronal Transient: Possible Evidence of Coronal Moreton Waves, *Astrophys. J.*, *517*, L151–L154.

Uralov, A. M., S. V. Lesovoi, V. G. Zandanov, and V. V. Grechnev (2002), Dual-filament initiation of a Coronal Mass Ejection: observations and model, *Solar Phys.*, *208*(1), 69–90.

Veselovsky, I. S., M. I. Panasyuk, S. I. Avdyushin et al. (2004), Solar and Heliospheric Phenomena in October-November 2003: Causes and Effects, *Cosmic Research*, *42*(5), 435–488.

Veselovsky, I. S., O. A. Panasenco (2002), Non-local dissipative structures in the solar corona: flaring loops, in *'From Solar Min to Max: Half a Solar Cycle with SOHO'*, Proc. SOHO 11 Symp. ESA SP-508, 461–464.

Webb, D. F., R. P. Lepping, L. F. Burlaga et al. (2000), The origin and development of the May 1997 magnetic cloud, *J. Geophys. Res.*, *105*, 27251–27260.

Wills-Davey, M. J. and B. J. Thompson (1999), Observations of a Propagating Disturbance in TRACE, *Solar Phys.*, *190*, 467–483.

Yermolaev, Yu. I., L. M. Zelenyi, G. N. Zastenker et al. (2005), Solar and heliospheric disturbances caused a strong magnetic storm on November 20, 2003, *Geomagnetism and Aeronomy*, in press.

Zarro, D. M., A. C. Sterling, B. J. Thompson, H. S. Hudson, and N. Nitta (1999), SOHO EIT observations of extreme-ultraviolet "dimmings" associated with halo coronal mass ejections, *Astrophys. J.*, *520*, L139–L142.

Zhitnik, I. A., O. I. Bougaenko, J.-P. Delaboudinière et al. (2002), SPIRIT X-ray telescope/spectroheliometer results, in *Solar variability: from core to outer frontiers*, Proc. of the 10th European Solar Physics Meeting, ESA SP-506, 915–918

Zhukov, A. N., F. Auchère (2004), On the nature of EIT waves, EUV dimmings and their link to CMEs, *Astron. Astrophys.*, *427*, 705–716.